

# Ruthenium (II) complexes of the chelating phosphine borane $\text{H}_2\text{ClB}\cdot\text{dppm}$

Nicolas Merle, Christopher G. Frost, Gabriele Kociok-Köhn,  
Michael C. Willis, Andrew S. Weller \*

*Department of Chemistry, University of Bath, Bath BA2 7AY, UK*

Received 11 November 2004; accepted 24 January 2005

Available online 17 March 2005

## Abstract

Reaction of  $\text{H}_2\text{ClB}\cdot\text{PPh}_2\text{CH}_2\text{PPh}_2$  ( $\text{H}_2\text{ClB}\cdot\text{dppm}$ ) with  $[\text{RuCp}^*(\text{NCMe})_3][\text{BAR}_4^{\text{F}}]$  ( $\text{BAR}_4^{\text{F}} = [\text{B}\{3,5\text{-(CF}_3)_2\text{C}_6\text{H}_3\}_4]^-$ ) results in displacement of all three acetonitrile ligands and the formation of  $[\text{RuCp}^*(\eta^2\text{-H}_2\text{ClB}\cdot\text{dppm})][\text{BAR}_4^{\text{F}}]$  (**1**), which has been characterised crystallographically. Reaction with carbon monoxide results in a change from  $\eta^2$  to  $\eta^1$  of the borane ligand to afford  $[\text{RuCp}^*(\text{CO})(\eta^1\text{-H}_2\text{ClB}\cdot\text{dppm})][\text{BAR}_4^{\text{F}}]$  (**2**). Compound **1** undergoes H/D exchange under a  $\text{D}_2$  atmosphere to afford  $[\text{RuCp}^*(\eta^2\text{-D}_2\text{ClB}\cdot\text{dppm})][\text{BAR}_4^{\text{F}}]$ , while **2** does not.

© 2005 Elsevier B.V. All rights reserved.

**Keywords:** Ruthenium; Borane; Hemi-labile; Co-ordinatively unsaturated

## 1. Introduction

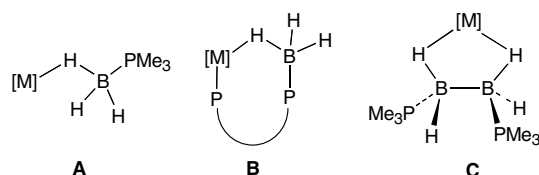
Phosphine boranes, such as  $\text{H}_3\text{B}\cdot\text{PR}_3$ , are valence isoelectronic with alkanes [1]. This relationship has been elegantly exploited by Shimoi in the isolation of analogues of elusive transition metal alkane complexes. For example,  $\sigma$ -alkane complexes such as  $\text{Cr}(\text{CO})_5$  (alkane) [2] and  $\text{ReCp}(\text{CO})_2(\text{C}_5\text{H}_{10})$  [3] have a limited lifetime and have only been characterised spectroscopically; while the related phosphine borane complexes, such as  $\text{Cr}(\text{CO})_5(\text{H}_3\text{B}\cdot\text{PMe}_3)$  [4] and  $\text{MnCp}(\text{CO})_2(\text{H}_3\text{B}\cdot\text{PMe}_3)$  [5] (structural type **A**, Scheme 1), are relatively stable at room temperature allowing them to be crystallographically characterised. However, these latter complexes are not completely robust and suffer from spontaneous decomposition, removal of the borane under a vacuum or substitution by another ligand, e.g. CO liberated in the initial synthesis [4].

Incorporating the borane into a bidentate, chelating ligand has the effect of stabilising the resulting complex towards loss of borane, in a similar manner to the stabilisation afforded to the  $\text{M}\cdots\text{H}_3\text{C}$  linkage in agostic complexes compared with intermolecular  $\sigma$ -complexes [6]. Thus, the chelating phosphine borane  $\text{H}_3\text{B}\cdot\text{PPh}_2\text{CH}_2\text{PPh}_2$  ( $\text{H}_3\text{B}\cdot\text{dppm}$ ) [7] (structure **B** Scheme 1) forms stable complexes that do not suffer from spontaneous decomposition or facile displacement of the  $\text{M}\cdots\text{HB}$  interaction. *Nido*- $\text{Rh}(\eta^2\text{-H}_3\text{B}\cdot\text{dppm})(\text{SB}_9\text{H}_{10})$  [8]  $\text{Cr}(\text{CO})_4(\eta^1\text{-H}_3\text{B}\cdot\text{dppm})$  [9],  $[\text{Rh}(\text{cod})(\eta^2\text{-H}_3\text{B}\cdot\text{dppm})][\text{PF}_6]$  [10] are examples of such complexes.<sup>1</sup> Coordination compounds of the chelating diborane ligand  $\text{B}_2\text{H}_4\cdot(\text{PMe}_3)_2$  (**C**) have also been reported, and this ligand can either adopt a monodentate or a bidentate binding mode such as  $\text{Cr}(\text{CO})_5\{\eta^1\text{-B}_2\text{H}_4\cdot(\text{PMe}_3)_2\}$  [1,11] and  $[\text{Cu}\{\eta^2\text{-B}_2\text{H}_4\cdot(\text{PMe}_3)_2\}_2]$  (**I**) [12]. We have

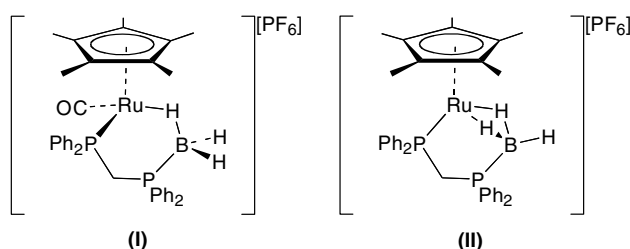
\* Corresponding author.

*E-mail address:* [a.s.weller@bath.ac.uk](mailto:a.s.weller@bath.ac.uk) (A.S. Weller).

<sup>1</sup> “ $\eta^x$ ” refers to the coordination mode of the phosphine–borane fragment with the metal centre. Implicit is that the other phosphine is always bound to the metal centre.



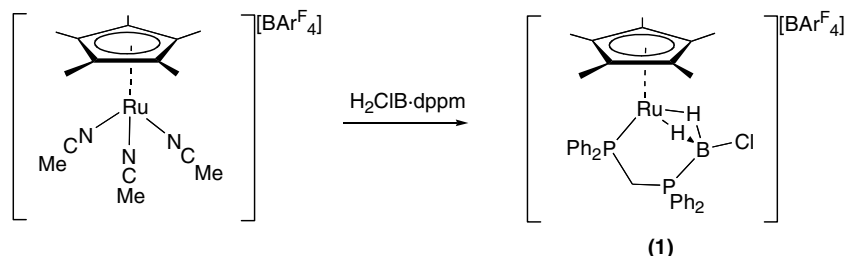
Scheme 1.



Scheme 2.

recently reported the synthesis, characterisation and reactivity of some ruthenium (II) complexes ligated with  $\text{H}_3\text{B}\cdot\text{dppm}$ . In these complexes, the phosphine borane can adopt either an  $\eta^1$  bonding mode, as in  $[\text{RuCp}^*(\text{CO})(\eta^1\text{-H}_3\text{B}\cdot\text{dppm})][\text{PF}_6]$  (**I**), or an  $\eta^2$  bonding mode,  $[\text{RuCp}^*(\eta^2\text{-H}_3\text{B}\cdot\text{dppm})][\text{PF}_6]$  (**II**) (Scheme 2). Complex **II** can be regarded as being “operationally unsaturated” in that the borane ligand can change from  $\eta^2$  to  $\eta^1$ , effectively providing a reactive 16-electron  $\{\text{RuCp}^*(\eta^1\text{-H}_3\text{B}\cdot\text{dppm})\}^+$  fragment. Indeed, addition of carbon monoxide to **II** cleanly affords **I**. This is similar to the way that borohydride and allyl ligands can change their coordination mode to reveal reactive, unsaturated, metal centres [13].

We are interested in extending this chemistry of ruthenium (II) fragments with chelating phosphine borane ligands to new ligand systems; and report here the synthesis of the new ligand  $\text{H}_2\text{CIB}\cdot\text{dppm}$  and its coordination with the  $\{\text{RuCp}^*\}^+$  fragment to form  $[\text{RuCp}^*(\eta^2\text{-H}_2\text{CIB}\cdot\text{dppm})][\text{BAR}_4^{\text{F}}]$  ( $\text{BAR}_4^{\text{F}} = [\text{B}\{3,5\text{-(CF}_3)_2\text{-C}_6\text{H}_3\}_4]^-$ ). Preliminary reactivity studies, including reaction with CO and  $\text{H}_2/\text{D}_2$  are also reported.



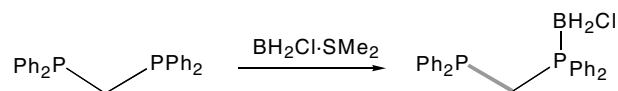
Scheme 4.

## 2. Results and discussion

The new, potentially chelating, phosphine borane ligand  $\text{H}_2\text{CIB}\cdot\text{PPh}_2\text{CH}_2\text{PPh}_2(\text{H}_2\text{CIB}\cdot\text{dppm})$  (Scheme 3) is readily synthesised by the addition of  $\text{BH}_2\text{Cl}\cdot\text{SMe}_2$  to  $\text{dppm}$  in toluene solvent. As for addition of  $\text{BH}_3$  to  $\text{dppm}$ , monofunctionalisation is clean, unlike that found in other bidentate phosphines such as  $\text{dppe}$  and  $\text{dppp}$  [7].  $\text{H}_2\text{CIB}\cdot\text{dppm}$  has been characterised by NMR spectroscopy and microanalysis. In the  $^1\text{H}$  NMR spectrum, the  $\text{BH}_2\text{Cl}$  group is observed as a quadrupolar broadened, integral 2-H, quartet at  $\delta$  3.93 [ $J(\text{BH})$  112 Hz] which sharpens somewhat in the  $^1\text{H}\{^{11}\text{B}\}$  NMR spectrum. The  $^{31}\text{P}\{^1\text{H}\}$  NMR spectrum displays two resonances at  $\delta$  3.7 and  $\delta$  -27.2. The latter is a sharp doublet [ $J(\text{PP})$  55 Hz] while the former is broad and is assigned to the phosphorus atom bound to boron. The  $^{11}\text{B}$  NMR spectrum shows a broad resonance at  $\delta$  -17.4; decoupling  $^1\text{H}$  reduces the line-width, but  $^{31}\text{P}\text{-}^{11}\text{B}$  coupling is not resolved.

Addition of  $\text{H}_2\text{CIB}\cdot\text{dppm}$  to  $[\text{RuCp}^*(\text{NCMe})_3][\text{BAR}_4^{\text{F}}]$  affords  $[\text{RuCp}^*(\eta^2\text{-H}_2\text{CIB}\cdot\text{dppm})][\text{BAR}_4^{\text{F}}]$ , compound **1**, in essentially quantitative yield (Scheme 4). Characterisation was by single crystal X-ray diffraction, NMR spectroscopy and microanalysis. Fig. 1 shows the solid-state structure of the cation, and Table 1 gives collection and refinement data.

The borane fragment in **1** adopts a bidentate bonding mode, with two bridging  $\text{Ru}\text{-H}\text{-B}$  3 centre–2 electron interactions, very similar to that observed in the analogous complex with  $\text{H}_3\text{B}\cdot\text{dppm}$ :  $[\text{RuCp}^*(\eta^2\text{-H}_3\text{B}\cdot\text{dppm})][\text{PF}_6]$  (**II**) [9]. The two bridging hydrogen atoms were located and refined, and the ruthenium–borane interaction is very similar in terms of bond lengths and angles to **II**. Thus the  $\text{Ru}\text{-H}$  distances in **1** [1.72(2) and 1.73(2) Å] are the same as found in **II** within error [1.61(4) and 1.70(3) Å]. The  $\text{Ru}\text{-B}$  distance is slightly shorter in **1**



Scheme 3.

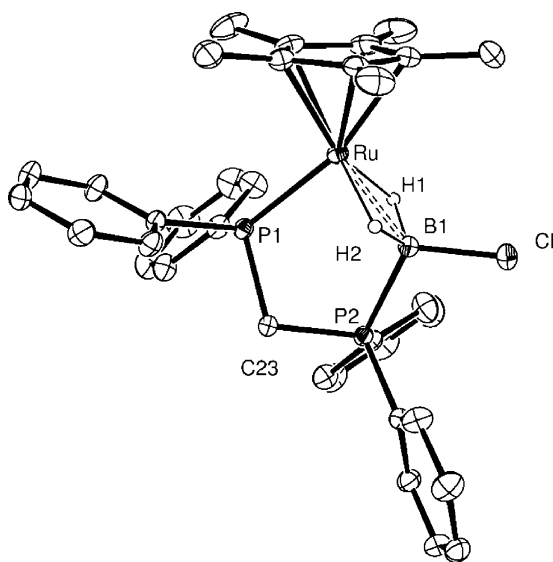


Fig. 1. Solid-state structure of the cationic portion of complex **1**. Hydrogen atoms, apart from those associated with the borane, have been omitted for clarity. Thermal ellipsoids are shown at the 30% probability level. Selected bond lengths (Å): Ru–B(1) 2.141(2), Ru–P(1) 2.3043(5), Ru–H(1) 1.72(2), Ru–H(2) 1.73(2), B(1)–P(2) 1.966(2), Cl–B(1) 1.806(1), B(1)–H(1) 1.28(2), B(1)–H(2) 1.32(3). Selected angles (°): B(1)–Ru–P(1) 87.80(5), Cl–B(1)–P(2) 131.73(10), B(1)–H(1)–Ru 89(1), B(1)–H(2)–Ru 88(1), B(1)–Ru–H(1) 36.7(8), B(1)–Ru–H(2) 37.9(9).

than in **II** [2.141(2) and 2.180(2) Å, respectively]. However, both these Ru–B distances are short, being comparable to that found in complexes with direct Ru–B  $\sigma$ -bonds [14]. Calculations on **II** [9] and related ruthenium hydridoborates [15] do indeed indicate a small, but significant, interaction between ruthenium and boron. Both B–H bond distances are in the range expected for a bonding B–H interaction. A significant B–H interaction is also indicated by the observation of B–H coupling in the  $^1\text{H}$  NMR spectrum (vide infra). The B–Ru–H angles ( $\sim 37^\circ$ ) are as expected for a dihydridoborate structure rather than a boryl/metal hydride in which these angles are substantially larger ( $60$ – $80^\circ$ ) [16]. The B–Cl bond length in **1** [1.806(1) Å] is unusually short for four-coordinate chloroboranes, viz. 1.83–1.90 Å. The two structurally characterised phosphine-mono-chloro boranes, both have significantly longer B–Cl bonds, viz.  $\text{BH}_2\text{Cl}\cdot\text{PPh}_2\text{BH}_2\text{PPh}_2\text{Cl}$ , 1.877(7) Å [17] and  $^t\text{Bu}_2\text{-PHBH}_2^t\text{Bu}_2\text{P}\cdot\text{BH}_2\text{Cl}$ , 1.898(4) Å [18]. This distance in **1** is also much shorter than in the complex  $\text{RuCp}^*(\text{PMe}_3)(\eta^2\text{-H}_2\text{BHCl})$ , 1.862(7) Å [19] which has a similar, dihydridoborate, structure to **1**. In fact, the B–Cl bond length is more like that found in metal complexes of three coordinate chloroboranes such as  $\text{FeCp}^*(\text{CO})_2\text{BClPh}$  [1.812(12) Å] [20] or  $\text{FeCp}(\text{CO})_2\text{-BCl}_2$  [1.781(3) Å] [21]. As expected the 4-methylpyridine adduct of this latter complex has a concomitantly longer B–Cl bond length [1.8853(14) Å]. Whether this short B–Cl bond length in **1** is indicative of B–Cl  $\pi$  overlap is not

Table 1  
Crystal data and structure refinement for compound **1**

Empirical formula	$\text{C}_{67}\text{H}_{51}\text{B}_2\text{ClF}_{24}\text{P}_2\text{Ru}$
Formula weight	1532.16
Temperature (K)	150(2)
Wavelength (Å)	0.71073
Crystal system	Triclinic
Space group	$P\bar{1}$
$a$ (Å)	12.54200(10)
$b$ (Å)	16.56200(10)
$c$ (Å)	17.46200(10)
$\alpha$ (°)	111.6770(10)
$\beta$ (°)	96.42
$\gamma$ (°)	93.76
Volume (Å <sup>3</sup> )	3327.07(4)
$Z$	2
Density (calculated) (mg/cm <sup>3</sup> )	1.529
Absorption coefficient (mm <sup>-1</sup> )	0.432
$F(000)$	1540
Crystal size (mm)	0.50 $\times$ 0.50 $\times$ 0.45
Theta range for data collection (°)	3.29–33.19
Reflections collected	68,934
Independent reflections	24,873 [ $R(\text{int}) = 0.0330$ ]
Absorption correction	Semi-empirical from equivalents
Data completeness	97.6
Refinement method	Full-matrix least-squares on $F^2$
Data/restraints/parameters	24,873/0/969
Goodness-of-fit on $F^2$	1.022
Final $R$ indices [ $I > 2\sigma(I)$ ]	$R_1 = 0.0447$ , $wR_2 = 0.1148$
$R$ indices (all data)	$R_1 = 0.0581$ , $wR_2 = 0.1260$
Largest diff. peak and hole (e/Å <sup>3</sup> )	1.722 and $-1.115$

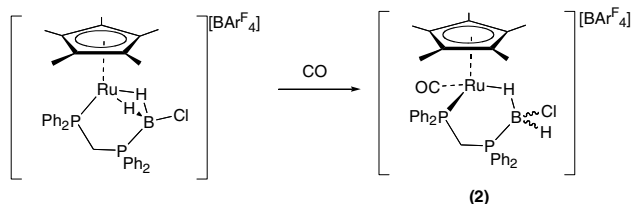
obvious, as compared with **II** (in which there are no  $\pi$  interactions) the Ru–B, Ru–H and B–P bond lengths are similar in both complexes.

In solution, the  $^{11}\text{B}\{^1\text{H}\}$  NMR spectrum of **1** shows a single resonance centred at  $\delta$  28.7, showing a significant downfield shift,  $\Delta\delta$  46.1, compared with free ligand, in concert with the short Ru–B distance observed in the solid state. This chemical shift change is similar to that observed for **II** compared with  $\text{H}_3\text{B}\cdot\text{dppm}$  [ $\Delta\delta$  55 ppm]. Similar magnitude chemical shift changes occur between  $\text{RuCp}^*(\text{PMe}_3)(\eta^2\text{-H}_2\text{BHCl})$  [19] and  $[\text{PPN}][\text{BH}_3\text{Cl}]$  [22] ( $\Delta\delta$  52 ppm). The signal in **1** is also a doublet, showing coupling to phosphorus [ $J(\text{PB})$  120 Hz], that resolves into a doublet of triplets in the  $^{11}\text{B}$  NMR spectrum [ $J(\text{HB})$  93 Hz]. By contrast, for the same signal in **II** these couplings are not resolved. The  $^1\text{H}$  NMR spectrum of **1** shows  $C_s$  symmetry is present in solution, with the methylene protons on the dppm backbone being observed as a relatively well defined, but still quadrupolar broadened, quartet at  $\delta$   $-8.87$  [ $J(\text{BH})$  93 Hz]. This is in contrast to **II** in which the B–H coupling is not resolved. The magnitude of the  $^{11}\text{B}$ – $^1\text{H}$  coupling constant in the  $\text{H}_2\text{ClB}\cdot\text{dppm}$  ligand has been reduced by 17% [112 vs 93 Hz] on coordination to the metal fragment, consistent with the description of the Ru–H–B bonding as 3

centre–2 electron. Similar-sized decreases in the B–H coupling constant have been noted for both mono-dentate and chelating phosphine boranes when coordinated with metal fragments [4,9].

In terms of the bonding between metal and borane fragment we have previously discussed this for **II**, and concluded that is best described as a dihydridoborate structure that has a significant Ru–B interaction [9]. The borane–metal bonding in **1** can be described in the same way, given the similar spectroscopic and structural characteristics between **II** and **1**.

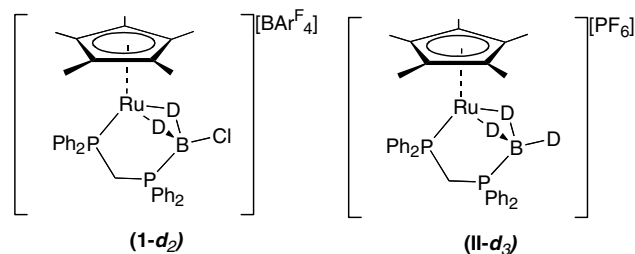
We have previously shown that the borane fragment in **II** can move from  $\eta^2$  to  $\eta^1$ , allowing two electron ligands to coordinate, such as MeCN, CO or  $\text{PMe}_3$  [9]. This change in bonding of the borane effectively makes the metal centre “operationally unsaturated”, revealing a latent 16-electron metal fragment. Similar reactivity is observed for **1**. Addition of CO affords  $[\text{RuCp}^*(\text{CO})(\eta^1\text{-H}_2\text{CIB}\cdot\text{dppm})][\text{BAR}_4^{\text{F}}]$  (**2**), which has been characterised spectroscopically by analogy with  $[\text{RuCp}^*(\text{CO})(\eta^1\text{-H}_3\text{B}\cdot\text{dppm})][\text{PF}_6]$  [9] (Scheme 5). In solution a quadrupolar broadened, high field signal is observed in the  $^1\text{H}$  NMR spectrum at  $\delta -9.47$ , of integral 1-H relative to the Cp\* resonance. This is assigned to the bridging Ru–H–B hydrogen. The methylene protons are now observed as two multiplets (d of d of d) showing that the  $C_s$  symmetry present in **1** has been lost on CO coordination. In the  $^1\text{H}\{^{11}\text{B}\}$  NMR spectrum the high field resonance sharpens and a new integral 1-H peak at  $\delta 1.85$  appears. We assign this to the terminal B–H. The observation of both terminal and bridging B–H in the room temperature NMR spectrum shows that they do not exchange on the NMR timescale. This is in contrast to **I**, in which rapid exchange of these groups occurs at room temperature. In the  $^{31}\text{P}\{^1\text{H}\}$  NMR spectrum a sharp signal at  $\delta 50.0$  and a broad signal at  $\delta 6.0$  are observed, the latter assigned to the boron-bound phosphorus atom. In the  $^{11}\text{B}$  NMR spectrum a broad signal is observed at  $\delta -18.2$  ppm, this being very similar to free ligand. This resonance is shifted 47 ppm upfield compared with **1**, demonstrating the structural change from  $\eta^2$  to  $\eta^1$  on reaction with CO. The IR spectrum shows a single CO stretching band at  $1908\text{ cm}^{-1}$  which is found to higher frequency than that for  $[\text{RuCp}^*(\text{CO})(\eta^1\text{-H}_3\text{B}\cdot\text{dppm})][\text{PF}_6]$  (**I**) ( $1963\text{ cm}^{-1}$ ) [9].



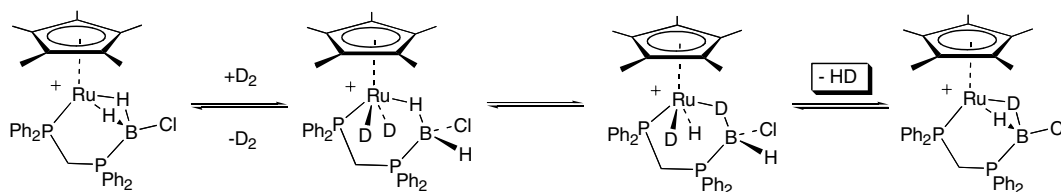
Scheme 5.

Addition of  $\text{H}_2$  to **1** (or **II**) does not result in any change in the  $^1\text{H}$  NMR spectrum either at ambient temperature or low temperature (200 K), initially suggesting no interaction of  $\text{H}_2$  with the metal centre. However, putting **1** (or **II**) under an atmosphere of  $\text{D}_2$  gradually (hours) results in the complete disappearance of the high-field bridging hydride signals in the  $^1\text{H}$  NMR spectrum. At the same time the  $^{11}\text{B}$  NMR spectrum of **1** changes from a doublet of triplets to a doublet at essentially the same chemical shift, indicating substitution of H for D. The B–D coupling, which would be significantly smaller ( $\sim 6$  times) than the B–H coupling, is not resolved. The  $^{31}\text{P}\{^1\text{H}\}$  NMR spectrum remains unchanged on treatment with  $\text{D}_2$ . This data show that H/D exchange is occurring in solution to afford  $[\text{RuCp}^*(\eta^2\text{-D}_2\text{CIB}\cdot\text{dppm})][\text{BAR}_4^{\text{F}}]$ , **1-d<sub>2</sub>** (Scheme 6). In the  $^2\text{H}$  NMR spectrum a single high-field resonance is observed at essentially the same chemical shift [ $\delta -8.85$ ] as found for **1**. Complete deuteration also occurs for **II** to afford **II-d<sub>3</sub>**.

H/D exchange in phosphine boranes has previously been observed in the  $\text{Re}(\text{PPh}_3)_2\text{H}_7/\text{H}_3\text{B}\cdot\text{PMe}_3$  system when heated in  $\text{C}_6\text{D}_6$  [23]. A mechanism that involves deuteration of a  $\{\text{Re}(\text{PPh}_3)_2\text{H}_5\}$  metal fragment by  $\text{C}_6\text{D}_6$  followed by the coordination of  $\text{H}_3\text{B}\cdot\text{PMe}_3$  and scrambling of hydrido and deuterio ligands has been described. No metal–borane intermediates, such as  $\text{Re}(\text{PPh}_3)_2\text{D}_5(\eta^1\text{-H}_3\text{B}\cdot\text{PMe}_3)$ , were observed however. A similar mechanism can be used to account for the H/D exchange observed in **1** and **II**, however in this case the metal–borane complex is well characterised (Scheme 7).  $\text{D}_2$  oxidatively adds to the Ru(II) centre in **1**, presumably initially through a dihydrogen adduct with a  $\eta^1$ -borane ligand. Oxidative addition of  $\text{H}_2$  to ruthenium (II) cyclopentadienyl phosphine complexes is known to form dihydride complexes such as  $[\text{RuCp}^*\text{H}_2(\text{P}^i\text{Pr}_3)_2][\text{BAR}_4^{\text{F}}]$  [24]. Breaking a B–H bond and making a B–D bond (similar to the exchange process observed in borohydride complexes such as  $\text{OsH}_3(\eta^2\text{-BH}_4)(\text{PR}_3)_2$  [25]) effects H/D exchange. Reductive elimination of  $\text{HD}_{(\text{g})}$  would then afford (initially partially) deuterated **1**. Experimentally, HD is observed [ $\delta 4.55$ ,  $J(\text{DH}) 43\text{ Hz}$ ] in the  $^1\text{H}$  NMR spectrum of **1** under a  $\text{D}_2$  atmosphere after 15 min. Consistent with this proposed mechanism, compound **2** is unchanged on exposure to  $\text{D}_2$  as it is



Scheme 6.



Scheme 7.

unable to generate an unsaturated species, which also has a coordinated borane – both being necessary for H/D exchange to occur. An alternative mechanism that involves initial oxidative addition of B–H to the metal (followed by H/D exchange with D<sub>2</sub>) has been discounted for related systems by Shimoi due to the high energy of the B–H σ\* orbital that would necessarily be involved in such a process [23,26]. Oxidative addition of three coordinate boranes to low valent transition metal centres is known [27].

### 3. Experimental

#### 3.1. General

All manipulations were carried out under an atmosphere of argon using standard Schlenk-line and glove-box techniques. Glasswares were predried in an oven at 130 °C and flamed with a blow-torch under vacuum prior to use. CH<sub>2</sub>Cl<sub>2</sub> and pentane were distilled from CaH<sub>2</sub>. CD<sub>2</sub>Cl<sub>2</sub> was dried over CaH<sub>2</sub> and distilled under vacuum. [RuCp\*(NCMe)<sub>3</sub>][BAR<sub>4</sub><sup>F</sup>] was prepared by salt metathesis of [RuCp\*(NCMe)<sub>3</sub>][PF<sub>6</sub><sup>F</sup>] [28] with K[BAR<sub>4</sub><sup>F</sup>] [29]. Microanalyses were performed by Mr. Alan Carver (University of Bath microanalytical service).

#### 3.2. NMR spectroscopy

<sup>1</sup>H, <sup>1</sup>H{<sup>11</sup>B}, <sup>11</sup>B, <sup>11</sup>B{<sup>1</sup>H} and <sup>31</sup>P{<sup>1</sup>H} NMR spectra were recorded on Bruker Avance 300 or 400 MHz spectrometers. Residual protio solvent was used as reference for <sup>1</sup>H and <sup>2</sup>H NMR spectroscopy (CH<sub>2</sub>Cl<sub>2</sub> δ = 5.32, CD<sub>2</sub>Cl<sub>2</sub> δ = 5.30). <sup>11</sup>B and <sup>31</sup>P were referenced to external BF<sub>3</sub>·OEt<sub>2</sub> and 85% H<sub>3</sub>PO<sub>4</sub>, respectively. Values are quoted in ppm. Coupling constants are given in Hertz. <sup>31</sup>P–<sup>1</sup>H coupling constants were deduced from <sup>1</sup>H{<sup>31</sup>P-selective} experiments.

#### 3.3. X-ray crystallography

The crystal structure data for **1** were collected on a Nonius-Kappa CCD diffractometer with details provided in Table 1. Structure solution, followed by full-matrix least-squares refinement was performed using the SHELXL suite of programs throughout [30]. Hydrogen atoms were included in calculated positions apart from

those associated with the borane which were located in the final difference map and refined without constraints. Crystallographic data files have been deposited with the Cambridge Crystallographic Data Centre (CCDC 255156), 12 Union Road, Cambridge CB2 1EZ (UK); Tel.: +44 1223 336 408, fax: +44 1223 336 033, e-mail: deposit@ccdc.cam.ac.uk.

#### 3.4. Synthesis

##### 3.4.1. H<sub>2</sub>CIB·dppm

Me<sub>2</sub>S·BH<sub>2</sub>Cl (0.115 g, 1.04 mmol) was added to a toluene solution of dppm (0.400 g, 1.04 mmol) and stirred for 1 h. Solvent was reduced in vacuo to minimum volume and layered with hexane. Storage at –30 °C over 3 days affords colourless crystalline material. Mass 0.355 g, yield 82%. C<sub>25</sub>H<sub>24</sub>BCIP<sub>2</sub> requires C, 69.40; H, 5.59. Found: C, 68.9; H, 5.72%. NMR data (all in C<sub>6</sub>D<sub>6</sub>) δ(<sup>1</sup>H): 8.32–6.86 (20H, m, Ph), 3.93 [2H, br q, BH<sub>2</sub>, J(BH) 112 Hz], 3.18 [2H, d, J(P(BH<sub>3</sub>)H) 10.5 Hz, CH<sub>2</sub>]. δ(<sup>1</sup>H{<sup>11</sup>B}) (selected): 3.93 (2H, br s, BH<sub>2</sub>). δ(<sup>31</sup>P{<sup>1</sup>H}): 3.7 (1P, br, P–B), –27.2 [1P, d, PPh<sub>2</sub>, J(PP) 55 Hz]. δ(<sup>11</sup>B{<sup>1</sup>H}): –17.4 (1B, br s, BH<sub>2</sub>Cl).

##### 3.4.2. [RuCp\*(η<sup>2</sup>-H<sub>2</sub>CIB·dppm)][BAR<sub>4</sub><sup>F</sup>] (**1**)

[RuCp\*(MeCN)<sub>3</sub>][BAR<sub>4</sub><sup>F</sup>] (0.150 g, 0.122 mmol) and H<sub>2</sub>CIB·dppm (0.053 g, 0.122 mmol) were stirred in 20 cm<sup>3</sup> of CH<sub>2</sub>Cl<sub>2</sub> for 30 min at room temperature. The solvent was removed in vacuo to leave red oil. Crystals suitable for an X-ray diffraction study were grown by dissolving the oil in minimum CH<sub>2</sub>Cl<sub>2</sub> and layering with pentane to yield red–orange crystals. Mass 0.177 g, yield 95%. C<sub>67</sub>H<sub>51</sub>B<sub>2</sub>ClF<sub>24</sub>P<sub>2</sub>Ru requires C, 52.52; H, 3.35%. Found: C, 52.70; H, 3.39%. NMR data (all in CD<sub>2</sub>Cl<sub>2</sub>) δ(<sup>1</sup>H): 7.86–7.20 (32H, m, Ph + BAR<sub>4</sub><sup>F</sup>), 2.96 [2H, dd, CH, J(PH), 8.8 Hz, J(P(BH<sub>3</sub>)H) 12.1 Hz], 1.62 (15H, s, Me), –8.87 [2H, br q, BH<sub>2</sub>, J(BH) 92.5 Hz]. δ(<sup>1</sup>H{<sup>11</sup>B}) (selected): –8.87 (2H, br s, BH<sub>2</sub>). δ(<sup>31</sup>P{<sup>1</sup>H}): 64.2 [1P, d, PPh<sub>2</sub>, Hz, J(PP) 83.3 Hz], 13.4 (1P, br, P–B). δ(<sup>11</sup>B): 28.7 [1B, dt, BH<sub>2</sub>Cl, J(PB) 120 Hz, J(HB) 93 Hz]. δ(<sup>11</sup>B{<sup>1</sup>H}): 28.7 [1B, d, BH<sub>2</sub>Cl, J(PB) 120 Hz], –6.6 (1B, s, BAR<sub>4</sub><sup>F</sup>). δ(<sup>2</sup>H): –8.85.

##### 3.4.3. [RuCp(CO)(η<sup>2</sup>-H<sub>2</sub>CIB·dppm)][BAR<sub>4</sub><sup>F</sup>] (**2**)

A CH<sub>2</sub>Cl<sub>2</sub> solution of [RuCp\*(η<sup>2</sup>-H<sub>2</sub>CIB·dppm)][BAR<sub>4</sub><sup>F</sup>] (0.100 g, 0.128 mmol) was stirred for 15 min under a CO atmosphere to give a yellow solution. Solvent



was removed in vacuo to leave a yellow solid.  $C_{68}H_{51}B_2ClF_{24}OP_2Ru$  requires C, 52.35; H, 3.29%. Found: C, 52.1; H, 4.01%. NMR data (all in  $CD_2Cl_2$ )  $\delta(^1H\{^{11}B\})$ : 7.75–6.97 (32H, m, Ph +  $BAr_4^F$ ), 3.61 [1H, ddd, CH,  $J(PH)$  10.9 Hz,  $J(P_{(BH_3)}H)$  10.9 Hz,  $J(HH)$  15.5 Hz], 3.30 [1H, ddd, CH,  $J(PH)$  7.7 Hz,  $J(P_{(BH_3)}H)$  14.7 Hz,  $J(HH)$ , 15.5 Hz], 1.85 (1H, br m, BH), 1.65 [15H, d, Me,  $J(PH)$ , 2.0 Hz],  $-9.47$  [1H, br s,  $BH_3$ ].  $\delta(^{31}P\{^1H\})$ : 50.0 [1P, d,  $PPh_2$ ,  $J(PP)$  44.8 Hz], 6.0 (1P, br, P–B).  $\delta(^{11}B\{^1H\})$ :  $-5.9$  (1B, s,  $BAr_4^F$ ),  $-18.2$  (1B, br). IR (KBr),  $\nu\text{ cm}^{-1}$ : 1980 (m, CO).

### Acknowledgements

The Royal Society and the EPSRC (GR/R90475/01) for support. Dr. John Lowe for assistance with recording the  $^2H$  NMR spectra.

### References

- [1] M. Shimoi, K. Katoh, Y. Kawano, G. Kodama, H. Ogino, *J. Organomet. Chem.* 659 (2002) 102.
- [2] C. Hall, R.N. Perutz, *Chem. Rev.* 96 (1996) 3125.
- [3] S. Geftakis, G.E. Ball, *J. Am. Chem. Soc.* 120 (1998) 9953.
- [4] M. Shimoi, S. Nagai, M. Ichikawa, Y. Kawano, K. Katoh, M. Uruichi, H. Ogino, *J. Am. Chem. Soc.* 121 (1999) 11704.
- [5] T. Kakizawa, Y. Kawano, M. Shimoi, *Organometallics* 20 (2001) 3211.
- [6] M. Brookhart, M.L.H. Green, L.L. Wong, *Prog. Inorg. Chem.* 36 (1988) 1; R.H. Crabtree, *Angew. Chem., Int. Ed.* 32 (1993) 789; G.J. Kubas, *Metal dihydrogen and  $\sigma$ -bond complexes*, Kluwer Academic Publishers, Dordrecht, 2001.
- [7] D.R. Martin, C.M. Merkel, J.P. Ruiz, *Inorg. Chim. Acta* 115 (1986) L29.
- [8] R. Macias, N.P. Rath, L. Barton, *Angew. Chem., Int. Ed.* 38 (1999) 162.
- [9] N. Merle, G. Kociok-Köhn, M.F. Mahon, G.D. Ruggiero, C.G. Frost, A.S. Weller, M.C. Willis, *Dalton Trans.* (2004) 3883.
- [10] M. Ingleson, N.J. Patmore, G.D. Ruggiero, C.G. Frost, M.F. Mahon, M.C. Willis, A.S. Weller, *Organometallics* 20 (2001) 4434.
- [11] M. Shimoi, K. Katoh, H. Ogino, *J. Chem. Soc., Chem. Commun.* (1990) 811.
- [12] M. Shimoi, K. Katoh, H. Tobita, H. Ogino, *Inorg. Chem.* 29 (1990) 814.
- [13] T.J. Marks, J.R. Kolb, *Chem. Rev.* 77 (1977) 263.
- [14] T. Yasue, Y. Kawano, M. Shimoi, *Chem. Lett.* (2000) 58; C.E.F. Rickard, W.R. Roper, A. Williamson, L.J. Wright, *Organometallics* 19 (2000) 4344.
- [15] K. Essalah, J.C. Barthelat, V. Montiel, S. Lachaize, B. Donnadieu, B. Chaudret, S. Sabo-Etienne, *J. Organomet. Chem.* 680 (2003) 182.
- [16] J.F. Hartwig, S.R. De Gala, *J. Am. Chem. Soc.* 116 (1994) 3661; D.R. Lantero, D.H. Motry, D.L. Ward, M.R. Smith III, *J. Am. Chem. Soc.* 116 (1994) 10811.
- [17] N.N. Greenwood, J.D. Kennedy, W.S. McDonald, *J. Chem. Soc., Dalton Trans.* (1978) 40.
- [18] H. Dorn, E. Vejzovic, A.J. Lough, I. Manners, *Inorg. Chem.* 40 (2001) 4327.
- [19] Y. Kawano, M. Shimoi, *Chem. Lett.* (1998) 935.
- [20] D.L. Coombs, S. Aldridge, S.J. Coles, M.B. Hursthouse, *Organometallics* 22 (2003) 4213.
- [21] H. Braunschweig, K. Radacki, F. Seeler, G.R. Whittell, *Organometallics* 23 (2004) 4178.
- [22] S.H. Lawrence, S.G. Shore, T.F. Koetzle, J.C. Huffman, C.-Y. Wei, R. Bau, *Inorg. Chem.* 24 (1985) 3171.
- [23] T. Kakizawa, Y. Kawano, M. Shimoi, *Chem. Lett.* (1999) 869.
- [24] H. Aneetha, M. Jiménez-Tenorio, M.C. Puerta, P. Valerga, V.N. Sapunov, R. Schmid, K. Kirchner, K. Mereiter, *Organometallics* 21 (2002) 5334.
- [25] I. Dewachy, M.A. Esteruelas, Y. Jean, A. Lledós, F. Maseras, L.A. Oro, C. Valero, F. Volatron, *J. Am. Chem. Soc.* 118 (1996) 8388; P.W. Frost, J.A.K. Howard, J.L. Spencer, *Chem. Commun.* (1984) 1362.
- [26] Y. Kawano, T. Yasue, M. Shimoi, *J. Am. Chem. Soc.* 121 (1999) 11744.
- [27] G.J. Irvine, M.J.G. Lesley, T.B. Marder, N.C. Norman, C.R. Rice, E.G. Robins, W.R. Roper, G.R. Whittell, L.J. Wright, *Chem. Rev.* 98 (1998) 2685.
- [28] B. Steinmetz, W.A. Schenk, *Organometallics* 18 (1999) 943.
- [29] W.E. Buschmann, J.S. Miller, *Inorg. Synth.* 33 (2002) 85.
- [30] G.M. Sheldrick, *SHELX-97*. A computer program for refinement of crystal structures, University of Göttingen.